

LA-UR-15-21096 (Accepted Manuscript)

Pressure-induced kinetics of the alpha to omega transition in zirconium

Jacobsen, Matthew
Velisavljevic, Nenad
Sinogeikin, Stanislav

Provided by the author(s) and the Los Alamos National Laboratory (2016-01-29).

To be published in: JOURNAL OF APPLIED PHYSICS ; Vol.118, iss.2, p.025902, JUL 14 2015

DOI to publisher's version: 10.1063/1.4926724

Permalink to record: <http://permalink.lanl.gov/object/view?what=info:lanl-repo/lareport/LA-UR-15-21096>

Disclaimer:

Approved for public release. Los Alamos National Laboratory, an affirmative action/equal opportunity employer, is operated by the Los Alamos National Security, LLC for the National Nuclear Security Administration of the U.S. Department of Energy under contract DE-AC52-06NA25396. Los Alamos National Laboratory strongly supports academic freedom and a researcher's right to publish; as an institution, however, the Laboratory does not endorse the viewpoint of a publication or guarantee its technical correctness.

Pressure-induced kinetics of the α to ω transition in zirconium

M.K. Jacobsen,¹ N. Velisavljevic,^{1, a)} and S.V. Sinogeikin²

¹⁾*Shock and Detonation Physics (WX-9), Los Alamos National Laboratory, Los Alamos, NM*

²⁾*HPCAT, Geophysical Laboratory, Carnegie Institution of Washington, Washington DC*

(Dated: 29 June 2015)

Diamond anvil cells (DAC) coupled with x-ray diffraction (XRD) measurements are one of the primary techniques for investigating structural stability of materials at high pressure-temperature (P-T) conditions. DAC-XRD has been predominantly used to resolve structural information at set P-T conditions and consequently provides P-T phase diagram information on a broad range of materials. With advances in large scale synchrotron x-ray facilities and corresponding x-ray diagnostic capabilities, it is now becoming possible to perform sub-second time resolved measurements on micron sized DAC samples. As a result, there is an opportunity to gain valuable information about the kinetics of structural phase transformations and extend our understanding of material behavior at high P-T conditions. Using DAC-XRD time resolved measurements, we have investigated the kinetics of the α to ω transformation in zirconium. We observe a clear time and pressure dependence in the martensitic α - ω transition as a function of pressure-jump, i.e. drive pressure. The resulting data is fit using available kinetics models, which can provide further insight into transformation mechanism that influence transformation kinetics. Our results help shed light on the discrepancies observed in previous measurements of the α - ω transition pressure in zirconium.

PACS numbers: 64.60.Ej, 64.60.fh, 62.50.-p

Keywords: Zirconium, High Pressure, Kinetics, Time Resolved

I. INTRODUCTION

At ambient pressure (P) and temperature (T), the group IV B metals titanium, zirconium, and hafnium are known to crystallize into the hexagonal close-packed α phase. These metals have been heavily investigated at high P-T conditions¹⁻¹² due, in part, to their importance for technical applications. In particular, zirconium is important as a component of nuclear reactors and is widely used for neutron work due to the low neutron cross-section. With the application of load, the α structure transitions to a more open hexagonal ω structure and the onset of this transition is highly influenced by the purity of the zirconium under investigation^{10,13,14}. From a mechanical point of view, the structural α to ω transition is of great importance, as the α phase shows a high degree of ductility and the ω phase is highly brittle at ambient conditions. However, there are currently several questions regarding the kinetics of this transition. To this end, we present work exploring the kinetics of the α to ω transition with *in situ* diamond anvil cell and x-ray diffraction experiments in the sub-second timescale.

A. Scientific Background on α - ω Transition in Zirconium

In terms of scientific interest, the α - ω relationship has been used widely to gain understanding of high pressure structural transformations, subsequent kinetics, and the influence of impurities on the phase boundary among

other aspects of the phase relationship. This intriguing transformation is even more interesting given that the ω phase is recoverable upon release of the applied load, which could point to competing thermodynamic stability between α and ω at ambient pressure. For example, can impurities stabilize or impede ω formation.

Although it is known that the martensitic α - ω transition occurs at high P-T, there are many remaining questions pertaining to this transition, including transition rate (i.e. kinetics), the effect impurities have on the volume change during transition, the transition pathways, or orientation relations. Initial work in this area focused on boundary and impurity effects^{5,15,16}, followed by some initial kinetics^{17,18}, and then orientation pathways via theoretical^{19,20} approaches. Recent experimental investigation has focused on the orientation relationships between α and ω . In a recent study¹¹, a dynamic multi-anvil (D-DIA) setup was used to investigate texturing of zirconium with pressure and experimentally concluded that previously suggested relations^{2,19} were at least partially correct. In these previous works, it was theoretically suggested, first for titanium² and later for zirconium¹⁹, that the transformation should be characterized by atomic shuffle and shear. In particular, Silcock's supposition was that the α to ω transition should be characterized by two orientation relationships that would define the transition. Wenk's¹¹ study used pole figures to investigate these possible relationships and found that one of these is applicable to the experimental results, supporting Silcock's theory in part.

However, such work has not resolved the debate surrounding the mechanism of this particular transformation. Initially, it was thought that the ω phase was the result of quenching the high temperature bcc phase (β)^{2,11},

^{a)}Corresponding Author: nenad@lanl.gov

but it was later demonstrated that it is a high pressure polymorph of the α phase^{1,3,5,11}. Further, this phase has been reported to occur under static conditions in the range from 4.6 (non-hydrostatic) to 6.4 (hydrostatic) GPa¹⁴. What is known regarding the mechanism of the α to ω transformation in zirconium is outlined well in the review by Hickman²¹ and in work by Trinkle²⁰ and Wenk¹¹. In these works, the ω phase is considered to form from conventional nucleation-growth and the fine scale of the resulting ω particulates suggest a homogeneous nucleation process via a direct transformation. In contrast, Jyoti *et al.* has suggested that the β phase⁸ appears as an unstable intermediary between the two and established a correspondence matrix between these transformations (α to β to ω). It should be noted that the existence of an intermediate phase has not been observed to date.

B. High Pressure Techniques for Kinetics Experiments

High-P experimental techniques can be generally described as either static (i.e. diamond anvil cell or DAC, multi-anvil press, etc.) or dynamic loading (i.e. gas gun, Z-pinch, etc.), whereas studies of the kinetics of such transitions, which are coupled directly to the mechanism, cannot be easily studied in either of these regimes. This is because kinetics studies require a well controlled, time-dependent change in thermodynamic variable across the sample followed by a static final condition for sample monitoring in near real time. Techniques for such studies have, until more recently, been widely unavailable or impractical to achieve. In the past, studies by Singh¹⁷, Davis and Adams²², and Brar and Schloessin²³ have been done with focus on reconstructive transitions. Historical reviews of this type of work are available from Onodera²⁴ and Osugi²⁵.

It is interesting to note the extent kinetic measurements have been applied to the study of materials, despite the difficulty of probing such states. For example, the initial attempts to incorporate kinetics measurements was primarily from geophysical studies and performed in large, multi-anvil setups²³ or were performed without the use of pressure²². The first effort to move beyond such large setups into pressure use and smaller table top setups was undertaken by Singh and colleagues in several experiments^{17,26–30}.

Initially, these experiments involved the rapid pressurization of a Bridgman-anvil type setup and continuous measurements of the sample electrical resistance, where pressurization was achieved through dropping a weight on the top of the cell. In later works, a system was developed to rapidly apply hydraulic pressure to this setup in a repeatable manner. From this, such experimentation progressed into the initial application of x-rays. However, there were severe time restrictions associated with such advances. For example, the technique discussed in Kruger's work³¹ suggests that the "rapid" time steps of

these experiments were of the order of 2-3 minutes. While no one would debate the rapidity of such measurements at the time, there are many transformations that are far too short to be probed at this time scale.

More recent studies involving high pressure jumps have aimed to probe the Grüneisen parameter of elemental metals^{32,33}. In these studies, temperature probes were included in the original Bridgman-anvil type setup and similar rapid hydraulic oil pressure jumps were used. Measurement was made of the pressure jump applied and the correlated temperature rise for a thermocouple embedded in the sample. These results were used with reference data to obtain estimates of the Grüneisen parameter over a limited pressure regime.

C. Theoretical Development for Kinetics Studies

With the exception of the most recent work, all such studies have attempted to analyze their results through the framework established by Avrami^{34,35}. In this, the composition of the resulting phase is plotted as a function of time, with the resulting form being

$$\omega(t) = 1 - \exp \{-(t/\tau)^n\} \quad (1)$$

with τ being the time constant of the transformation and n being the associated exponent. In the original work of Avrami³⁵, he states that the exponent only exists in integer form (i.e. $n = 1, 2, 3, 4$) and is associated with the dimensionality of the growth stage of the resulting phase. For example, a exponent of three would correspond to planar restricted growth of the daughter phase. Extensions have been made to obtain more information than just the time constant and exponent alone would allow. Singh¹⁷ suggests that the activation free energy associated with the transformation can be obtained from the time constant of the transformation, which will be discussed in more detail later in this report.

In contrast, one assumption of the Avrami model is that nucleation and growth occur from the center region of a crystallite. The validity of this statement is not questioned here. There is the possibility, as was raised by Clemm and Fisher³⁶, that such nucleation and growth could occur from grain boundaries or corners as well. Such a consideration was taken into account by Cahn³⁷, where he showed that such considerations required no modification to the Avrami form above. What he did find was that the restriction on the exponent should be relaxed to allow for non-integer values. Such a determination has the experimental support of all references found on this topic, where the exponent is routinely between integer values. Unfortunately, such experimental results raise the additional problem of sub-unity values for the exponent, as neither Avrami's nor Cahn's theoretical bases cover such a situation.

Despite this previous work, the extent of application for such kinetics studies has been restricted due to the lack of direct probes of structure with pressure and time.

In the past decade, high pressure science has seen the introduction of techniques for rapidly increasing pressure in a controllable fashion^{9,38} and a dramatic increase in the speed of x-ray sources and detectors. With the recent or pending upgrade of several central user x-ray sources, it is becoming increasingly possible to investigate such transitions and gain insight into the fundamental mechanisms of transformation. Furthermore, such studies are imperative to enhance our understanding of the kinetics of these transitions. For example, the previous studies from Singh¹⁷ are analyzed under the assumption of complete transformation between phases, while there is no direct measure to support this in those works. When combined with x-ray studies, it becomes possible for the first time to determine the ratio of the initial and final phases and better quantify this transition.

II. EXPERIMENTAL DETAILS

As discussed, the effect that impurities have on the zirconium phase transition pressure has been previously investigated^{10,14,39}. In particular, it is known that commercial purity zirconium exhibits the α to ω transition between five and six GPa higher than the highest purity material, depending on the hydrostatic nature of the experiment. As the applicability of the results to the phase diagram depends largely on the sample condition, all work done in this report was performed on the same highest available purity zirconium as was used in previously published works^{14,39}.

Experiments were undertaken at the Advanced Photon Source at Argonne National Laboratory, using the facilities of Sector 16 (HPCAT, ID-B beamline). All x-ray diffraction measurements were angle dispersive with a wavelength of 0.406626 Å and a spot size of 5x3 μm, which was centrally located on the sample region for non-hydrostatic experiments. X-ray patterns were collected using a Pilatus 100k area detector. Samples were studied both hydrostatically (4:1 Methanol:Ethanol medium) and non-hydrostatically (no pressure medium) with copper powder included for pressure determination. All samples were loaded in stainless steel 301 gaskets with a 150 μm hole.

These prepared cells were coupled to a piezoelectric module, recently adapted for high-P work at HPCAT, for rapid increase. This module consists of an annular piezoelectric and a container to hold the piezoelectric against the piston of a DAC. The piezoelectric is actuated by a coupled power supply and waveform generator, located outside the experiment hutch. In this case, the voltage applied to the piezoelectric was step increased, actuating the piston side of the DAC and effecting a quick pressure change. For consistency, all samples were initially pressurized slowly until the starting pressure in the cell was between 0.5 and 4.5 GPa. At this point, the piezoelectric module was used to apply a rapid pressure increase (< 0.1 seconds) while collecting x-ray diffraction spectra *in situ*

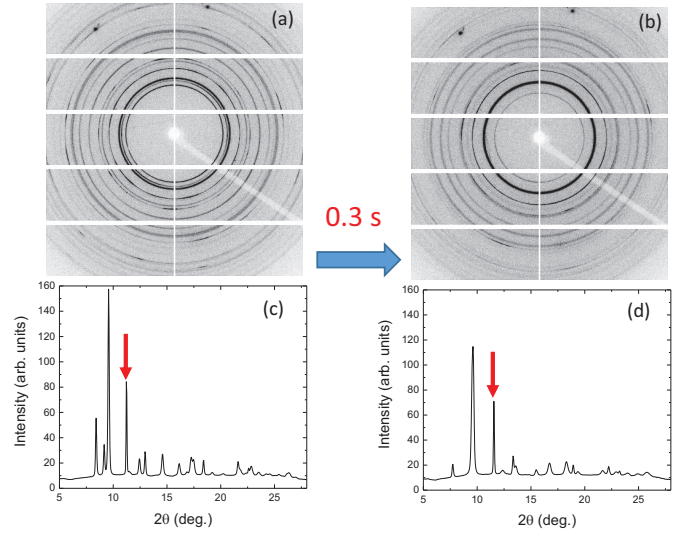


FIG. 1. Representative examples of x-ray diffraction patterns obtained for zirconium with a copper pressure marker. This data was collected from one of the non-hydrostatic runs (16.7 GPa) and shows the patterns before (a and c) and after (b and d) the piezoelectric element was triggered. Prior to triggering the piezoelectric, the pressure was 2.27 ± 0.08 GPa (a and c) and after the pressure was 16.7 ± 0.5 GPa. The [111] copper peak is indicated in each by the arrow, with a total of four copper peaks existing in the range of diffraction available and used for indexing. (Color online.)

at 0.1 seconds per pattern. It should be noted that when the term pressure jump or ramp or increase is used, it refers to a change in the sample pressure measured while voltage is applied on the piezo-element.

III. RESULTS

Data was converted to 2θ versus intensity using Fit2D, with examples of the raw images and converted patterns shown in Figure 1, and Rietveld pattern fitting was performed using MDI's Jade. In this refinement, CIF files of all phases (α and ω zirconium and copper) were used from the ICSD database to fit the initial structure, with the background fit using a polynomial.

An example of one such refinement is shown in Figure 2. A Pearson-VII function was used to fit the peak shape with the full width at half maximum refined individually for each peak. Structural refinement of the copper pressure marker, including all four peaks that were in the two-theta range of this experiment, were used to determine pressure⁴⁰.

Phase fractions were extracted from the Rietveld results based on relative peak intensities and are plotted as a function of time in Figure 3. Data shown in this figure is from all experiments that did not have instantaneous transformations (< 0.1 sec). A list of the experiments

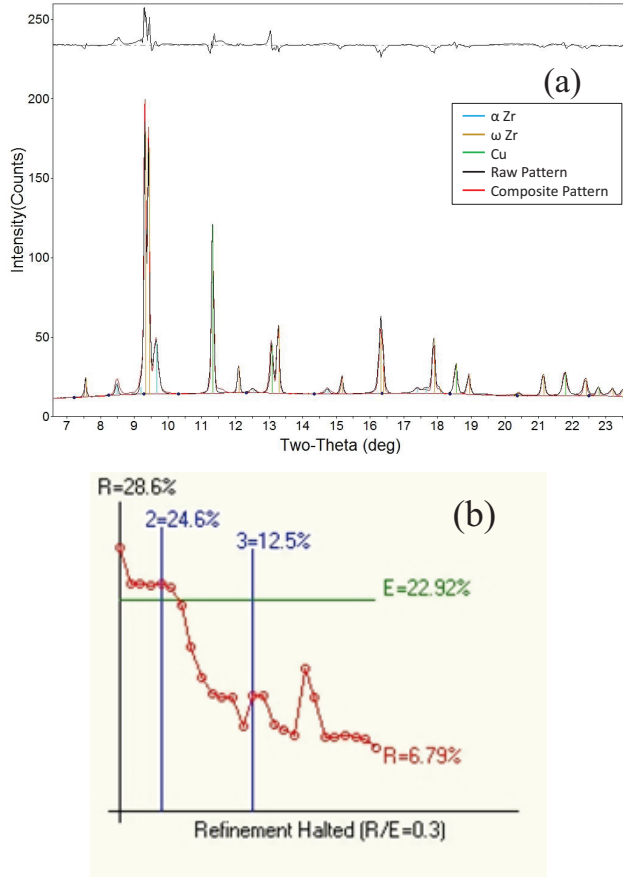


FIG. 2. Example refinement plot (a) for a representative x-ray pattern. In this plot, the composite curve is constructed of refined cell parameters, atomic positions, and peak shapes for copper and α and ω zirconium, along with a polynomial background. In this plot, the pattern was for Experiment 7 and 5.6 ± 0.2 GPa. Residuals for the curve are shown at the top of the plot. The R-value (b) of the fit reaches approximately 6.8%, indicating a reasonably good fit. (Color online.)

performed are shown in Table I.

In addition to the Avrami fits, x-ray patterns can be used to demonstrate the temporal evolution with lack of pressure evolution. An example for this is shown in Figure 4, where patterns have been plotted as a function of time from voltage being applied to the piezoelectric element. This shows clearly that the pressure does not fluctuate to any noticeable degree, but evolution of the ω phase occurs over this same time period.

IV. DISCUSSION

The resulting composition versus time data can be analyzed through the frame work developed by Avrami^{34,35} with application to high-P structural transformations discussed in other works^{17,22,23}. However, there are several assumptions used in the derivation. The most ini-

TABLE I. Experimental Details for Rapid Compression Experiments at the APS. H and NH stand for hydrostatic and non-hydrostatic loading, respectively. Strain rate is calculated from the Cu phase volumes prior and after the pressure jump and the spectra time delay (0.1 s). TTS refers to the transtion time scale and measures the length of time between the start of the pressure jump and when a stable composition is reached. Errors for the values in this table are in parentheses after the digit it corresponds to.

Start P (GPa)	Final P (GPa)	Loading	$\dot{\epsilon}$ (1/s)	TTS (s)	Exp. #
4.2(1)	7.9(2)	H	0.1354	8	3
4.1(1)	13.8(6)	H	0.6372	± 0.1	4
0.5(1)	13.5(5)	H	0.6221	± 0.1	5
0.8(1)	5.5(2)	NH	0.2986	400	1
4.5(1)	5.9(2)	NH	0.0706	300	7
4.4(1)	9.4(2)	NH	0.2362	70	6
2.3(1)	16.7(5)	NH	0.4611	± 0.1	2

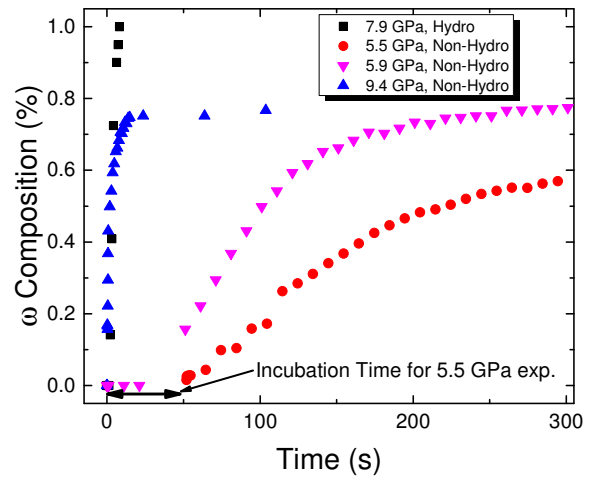


FIG. 3. Temporal evolution of ω phase for non-instantaneous transformations. Pressure jump and hydrostatic condition for sample is indicated in the legend. In this case, hydrostatic (hydro in the legend) refers to a 4:1 Methanol to Ethanol mixture surrounding the sample, where non-hydrostatic (non-hydro) indicates only powdered sample loaded. Pressure is determined from co-loaded copper marker. Error is represented by the size of the symbols.

tially relevant assumption is that of total conversion of the resulting material. As seen in Figure 3, non-hydrostatic loading, as determined by x-ray diffraction, results in less than full conversion over the span of measurement (≈ 5 minutes).

To account for this, there are two possible approaches. The first would be normalizing the resulting information to extract only the Avrami related parameters from the fit. The second method would be to add a scale factor into the Avrami equation itself. In our approach, the second of these options is used, as the conversion percentage could be useful in addition to the Avrami parameters. As such, this modification (A prefactor in Eq. 2) results in

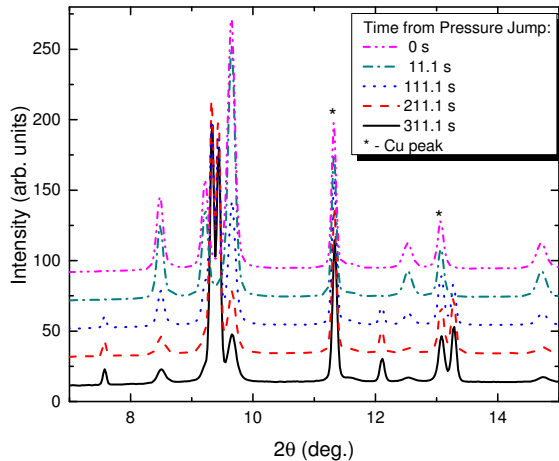


FIG. 4. Example x-ray spectra (5.9 GPa for all curves shown) for temporal progression of ω phase from Experiment 7 (5.9 GPa). Specific details of the fit are discussed in the text, but it is important to note the incomplete conversion, as is shown in the x-ray patterns. (Color online.)

the form

$$\omega(t) = A(1 - \exp\{-(t/\tau)^n\}). \quad (2)$$

where $\omega(t)$ is the percentage of ω phase as a function of time, τ is the characteristic time of the transformation, and n is an exponent related to the dimensionality of the transformation. Forms similar to this have previously been applied to describe incomplete transitions⁴¹.

Beyond just the full conversion assumption, Avrami's formalism specifically limits the exponent to integer values. However, there is a substantial amount of evidence that such a restriction prevents adequate analysis of the resulting data^{17,27,29,41}. Thus, for the purposes of analysis here, this assumption has been relaxed also. The resulting analysis then becomes more similar to that put forward by Cahn³⁷. To expand on the previous definitions, this suggests regions of nucleation/growth covering dimensionality from three ($n=4$) to zero ($n=1$). In addition, mixed regions can occur, which can give a hint as to what type of growth is occurring. For example, an exponent of 3.65 would correspond to a majority of three-dimensional growth, but with some planar growth or nucleation in addition. In our interpretation, this appears to be a much more reasonable take on the transformation process, as it allows for all possible nucleation and growth mechanisms to be present.

Other formalisms and theoretical bases exist for such analysis, such as that developed by Sung and Burns⁴². In their work, they derive a very detailed form, involving numerous constants for fitting. Further, they divide the transformed volume versus time function into two regions, one prior to site saturation and one subsequent. While very detailed, their form is essentially a more specific version of the Avrami equation. However, they suggest that prior to site saturation the exponent n should be restricted to 4 and 1 after saturation is achieved.

TABLE II. Results of data fits to modified Avrami equation (Eq. 2). A is the conversion limit pre-factor included in the modified form and Inc. time is the incubation time. All units are presented in parenthesis. Results are listed for hydrostatic experiments first, followed by non-hydrostatic experiments in increasing final pressures.

Final P (GPa)	τ (s)	Exp.	A (%)	Inc. Time (s)	ΔG (eV/atom)
7.9(2)	3.77(5)	3.38(2)	100	1.2(1)	0.509(1)
5.5(2)	149(1)	2.48(6)	55.4(5)	51.7(1)	0.605(2)
5.9(2)	99(2)	1.85(6)	75.1(8)	21.1(1)	0.594(3)
9.4(2)	0.15(3)	0.44(7)	91(1)	0.0(1)	0.427(2)

From any of these forms, it is possible to extract an estimate of the activation energy barrier (ΔG^*) in a similar method to that described by Singh¹⁷. Starting with the time constant for the transformation process, the relation is

$$\ln \tau = b_0 + \frac{\Delta G^*}{RT} \quad (3)$$

where b_0 is a constant, R is the gas constant, and T is the temperature. When there is no activation energy, theory suggests that the transformation will propagate at the speed of sound, which allows the constraint of possible values for b_0 , if the sound speed is known. For the case of zirconium, it has been previously measured in this pressure regime⁷ to be approximately 4.8 km/s. Using the initial gasket thickness of 50 μm , the time for this wave to traverse the sample is approximately 10 ns and gives an upper bound for the b_0 parameter of -18.4, which is then used to determine the activation energy barrier from the time constants. Beyond just the model used for fitting the transformed fraction curve, it is common to determine the so-called incubation time. This is not a fitted parameter and is defined simply as the region of indifference of the transition (i.e. the temporal region where no change is observed upon jumping the pressure)^{5,17,27,29}, as indicated in Figure 3.

An example of the modified Avrami fit is shown in Figure 5. The results of fitting with this form are shown in Table II, along with estimated values of the activation barrier at each jump pressure and values of the so-called "incubation" time. One interesting feature is the dramatic rise in conversion percentage with a relatively small additional load. Along with this, zirconium undergoes an incomplete transformation under non-hydrostatic conditions up to at least 9.4 GPa, above which a full 100% conversion to the omega phase is observed.

The results of our work also show no evidence of the supposed α - β - ω transition chain, previously supposed by Jyoti *et al.*⁸. Further, previous kinetics measurements using electrical resistivity probes¹⁷ illustrate only the direct conversion (single resistive jump) between these two phases. As such, this data suggests that this supposed transition mechanism is not likely.

A decaying exponential relation between the incubation time and the maximal conversion percentage is also

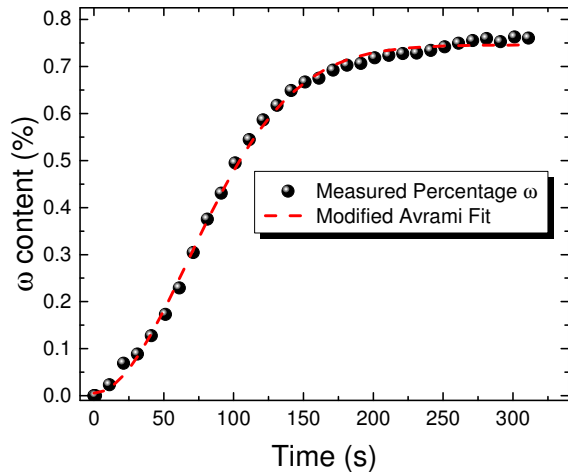


FIG. 5. Example fit of pressure jump data using modified Avrami equation from Experiment 7 (5.9 GPa) and associated x-ray spectra (5.9 GPa for all curves shown). Specific details of the fit are discussed in the text, but it is important to note the incomplete conversion, as is shown in the x-ray patterns. The exponent for this experiment was 1.85(6), suggesting a combination of one dimensional and point conversion. (Color online.)

evident from the data. It has been previously discussed that the incubation time can be considered an inherent transition property¹⁷ and could be related to embryo development⁴³. It would then appear that there is some relation between the time required to form embryos and the extent of propagation in transformation.

Both the time constant and the Avrami exponent for non-hydrostatic experiments show a rapid decrease with increasing pressure. The time constant relation would be expected as a larger overdrive of the applied load would result in each grain reaching the critical pressure more rapidly. The exponent results are more surprising. Based on the previous interpretations of the exponent, a decreasing exponent suggests a decreasing dimensionality of the transformation. Thus, a larger overshoot of transition pressure results in a more spontaneous and localized transformation of material from α to ω .

The activation barrier determined from these results shows a similar trend, with a steady decrease with applied pressure. In contrast, it has been previously reported, based on reversion studies¹⁸, that the activation energy for the ω to α backtransformation increased with the maximal load applied to the material. Samples used in the reported experiments¹⁸ were initially of high purity and shocked to either 8.5 or 10 GPa. The recovered samples were then heated while using x-ray diffraction to determine reversion time constants. The authors reported that the activation energy for the backtransformation increased from 1.05 eV to 1.73 eV between the two samples, with higher applied load resulting in the higher energy. However, our analysis suggests the activation energy for the forward transformation decreases with in-

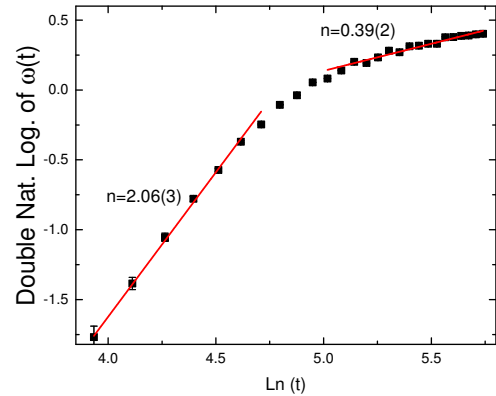


FIG. 6. Example fit (Exp. 7, 5.9 GPa) using Cahn's proposed form (Eq. 4). In this form, the data should form regions corresponding to different rates and growth dimensionality. The results from our analysis demonstrate that the suggestion by Sung⁴² is likely not appropriate here. Instead of the $n=4$ and $n=1$ regions suggested, we find that the exponent values are routinely less than this, suggesting restricted growth. However, as noted in the text, the determination of independent regions is left to the judgment of the data processor. As such, the results of such analysis must be treated with caution.

creasing load at $0.05 \frac{eV}{GPa}$, suggesting that the activation barrier would disappear around 19 GPa. This should not be confused with the location where near instantaneous transformation appears to occur, which from our results would be between 10 and 13 GPa. Such a result is not surprising, as it is known that this transformation introduces texturing that is irreversible and would likely effect the reversion energy¹¹.

Another method of analysis is suggested by Cahn³⁷, where inspection of logarithmic relations of the form

$$\ln \ln \frac{1}{1 - \omega(t)} = \ln K + n \ln t \quad (4)$$

may provide useful information. In this equation, K is a rate constant and n is the Avrami exponent. When converted to this form, each curve shows regions approximating a linear rate, as shown in Figure 6, but with highly varying Avrami exponent values. There are several implications to this. First, the proposition by Sung⁴² that each transformation can be divided into a region of $n=4$ and $n=1$ does not seem to be applicable here, as is seen in Figure 6 for Experiment 7 (5.9 GPa). Analysis of this sort was performed, with the regions being limited to two and requiring the temporal ends to be used in one of the two regions. The results of this are shown in Table III.

While the Cahn fits can be seen to allow deeper analysis than Avrami's, there is a certain degree of flexibility in the interpretation of these results, as there are no restrictions to the placement of the fit regions. In contrast, by dividing the Cahn curve into regions, different processes can be resolved allowing some insight to be gained

TABLE III. Results of data fits to Cahn’s proposed form (Eq. 4). These results correspond to a fit at the beginning of the curve and end of the curve. Errors for the exponent are shown in parentheses next to the digit they correspond to. The rate constants (RC) are determined by exponentiation of the intercept (B) (i.e. $RC = \exp(B)$). Results are listed for hydrostatic experiments first, followed by non-hydrostatic experiments in increasing final pressures.

Final P (GPa)	Rate Constants ($10^3/s$)	Exponents
7.9(2)	11.2 - 130	3.30(1) - 1.58(4)
5.5(2)	0.005 - 7.99	2.3(2) - 0.83(2)
5.9(2)	0.054 - 201	2.06(3) - 0.39(2)
9.4(2)	1761 - 1942	0.37(1) - 0.11(1)

into the internal transformations and how they occur. As such, caution is recommended when using Cahn’s proposal for analysis. These results show similar results to the modified Avrami model in that higher final pressures correspond to more rapid transformation.

As for the dimensionality, the hydrostatic (7.9 GPa) experiment shows an initial combination of three and two dimensional conversion, with primarily two dimensional character. From the modified Avrami results (Exp. 3, 7.9 GPa), hydrostatic conditions show an exponent ($n=3.38(2)$), in agreement with the result from Cahn’s proposed analysis above. While it might be initially assumed that a three dimensional conversion should appear, as this is hydrostatic, it is known that zirconium’s α to ω transition is at least aided by shear⁴⁴. As a result, the transformation would be more likely to show some two dimensional character, which is suggested by an exponent of three. There is obviously more than just shear present though, as the mixed character also suggests some three dimensionality to the transformation, which may be consistent with atomic shuffle. An independent, direct measurement under dynamic loading conditions (similar to that done for static pressure¹¹) is needed to better confirm the transformation mechanism.

The exponents from both fitting methods indicate a lower dimensionality for non-hydrostatic conversion than the hydrostatic case. Results from work by Errandonea⁴⁴ and Sikka¹⁵ have previously demonstrated the influence that non-hydrostatic conditions can have on this transition. In particular, Sikka postulates that retention of a completely transformed ω phase at ambient pressure is only possible if the uniaxial component of the pressure is very small compared with the hydrostatic component (i.e. $P_{uni} \ll P_{hydro}$). The work from Errandonea demonstrates that less hydrostatic pressure media result in partial conversion. So, the more hydrostatic the conditions are, the more likely the sample will completely convert to ω . In contrast, a higher uniaxial stress component results in incomplete conversion. It is known that non-hydrostatic compression often results in texturing¹¹, with grains orienting along the minimum stress directions and reducing the internal stress in the material. Such a reduction in stress may also impede progression of the

transformation, requiring higher applied load to complete the transition. Similar results are found in multiple shock experiments studying this transformation^{18,45–47}.

However, interpretation of these remains a challenge. As has been mentioned in previous works^{17,27,29}, one important improvement to make is to formulate a theoretical explanation for the sub-unity exponents seen. From the results of this work, it can be said the sub-unity values of the exponent are required to accurately and completely characterize the transformation kinetics. Returning to the dimensionality arguments suggested in Avrami’s original work^{34,35}, a sub-unity transformation rate is more likely to suggest isolated transformations in a sea of untransformed material. Since the exponent is an *average* measure of the nucleation and growth rates of the whole of the material, this anomaly is possibly related to the assumption of constant nucleation and growth rates. To better explore this possibility, it would be necessary to probe individual grains to monitor the progression of the transformation in each type of loading.

In addition, it is important to distinguish between sample and experimental effects. For example, the internal pressure drift as a result of the rapid loading can be considered to cause early or partial transformation of the sample. To investigate this possibility, Figure 7 shows the change in pressure over the experiment period for representative hydrostatic (Exp. 3, 7.9 GPa) and non-hydrostatic (Exp. 7, 5.9 GPa) samples. In this, the pressure variation is on the order of 0.5 GPa for non-hydrostatic loadings and 0.25 GPa for hydrostatic in the stable region.

Further evidence can be found through examination of the unit cell volumes as a function of time for the same samples. This is shown in Figure 8, where it is seen that after a brief period of change, the unit cell volume stabilizes for the remainder of the experiment period. Along with the volume change as a function of time, these plots also show the full width at half maximum of the $[1\ 0\ 0]$ peak for α zirconium and $[0\ 0\ 1]$ peak for ω zirconium. In the hydrostatic, no difference is seen between the two phases and the trend shows little change, whereas the non-hydrostatic shows a slight increasing trend indicating more non-hydrostatic conditions as the transformation progresses. As a result, we consider these to be insubstantial effects and their impact as a driving factor for this transition is disregarded.

V. CONCLUSIONS

In conclusion, we report on studies of the effect of rapid loading on zirconium’s α to ω phase transition using *in situ* x-ray diffraction measurements coupled with diamond anvil cell compression. Specifically, we have investigated the kinetics of the transformation and the dependence of the transformation rate on sample hydrostaticity. The most important result of this work is the clear demonstration of the capacity to perform such

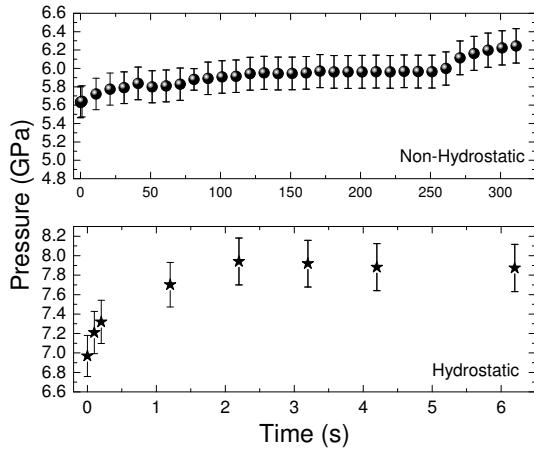


FIG. 7. Temporal evolution of internal pressure for both hydrostatic (Exp. 3, 7.9 GPa) and non-hydrostatic (Exp. 7, 5.9 GPa) experiments, as determined by Cu internal calibrant. It is clear from this that the pressure is stable within 0.5 GPa for non-hydrostatic and 0.25 GPa for hydrostatic after a brief increasing region. The magnitude of this fluctuation is of similar order for all experiments.

measurements on a sub-second timescale with *in situ* x-ray diffraction. *In situ* x-ray diffraction measurements provide a direct measure of phase ratio and our results further add to previous work, which was most often performed using electrical resistivity as a probe^{17,26,29,30}. Despite the very thorough experimentation and analysis performed in these works, electrical resistivity is a secondary probe with no direct determination that the sample has made a complete transition between the phases under study. In contrast, our work deduces similar information from a direct probe, allowing experimental determination of the phase ratio.

Beyond this step forward in the study of kinetics, the results of this work support the conclusion that there is likely not an intermediate phase occurring between the α and ω phases, as has been previously supposed⁸. X-ray patterns obtained in this work have shown no evidence of the high pressure β phase occurring and previous resistive measurements show evidence of only a single transition^{17,48}.

Further experimental development is required to help better determine the physical meaning of the fit exponents and how far the proposed models extend. For example, while the current data suggests a direct transformation from α to ω , it does not resolve the pathway taken to achieve this. Due to the averaging nature of the data collected ($5 \times 3 \mu\text{m}$ window), it is impossible to extrapolate from this to nucleation or growth methods that individual grains undertake, which would be necessary to obtain such information. An additional complication exists from the stress state of the material. Non-hydrostatic samples will exhibit pressure differentials based on the shear strength of the material, which

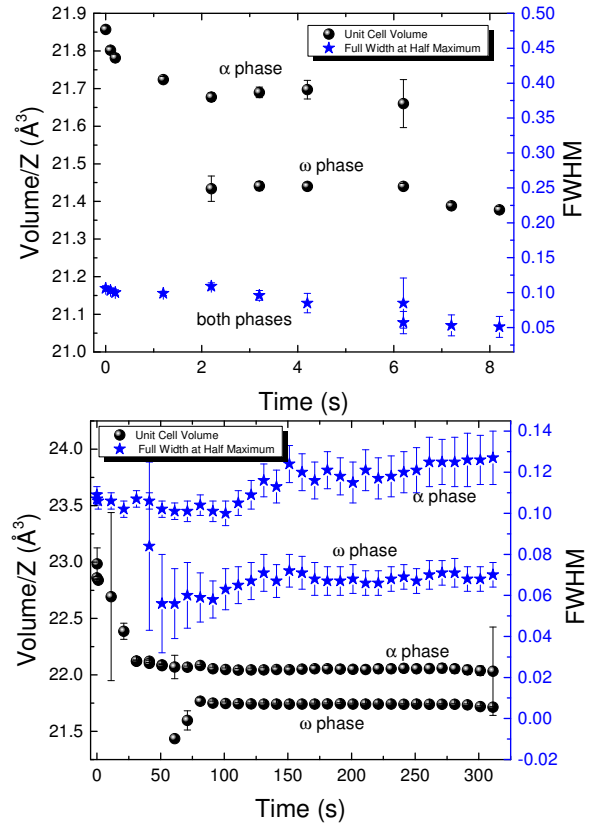


FIG. 8. Temporal evolution of unit cell volume and full width at half maximum for both hydrostatic (Exp. 3, 7.9 GPa) and non-hydrostatic (Exp. 7, 5.9 GPa). In these, the full width at half maximum is plotted for the $[1\ 0\ 0]$ peak for the α phase and the $[0\ 0\ 1]$ peak for the ω phase. As the magnitude of the fluctuation of either of these parameters is generally within the error, it can be assumed that any pressure drift has little effect on the progression of the transformation. (Color online.)

can alter the transformation and texture of the resulting material. Such conditions also complicate the physical origin of the transformation. It can be argued, based on stress analysis of the sample region in a DAC, that the highest stress state is centrally located on the anvil surfaces. However, a high shear state will exist in a non-hydrostatic sample near the boundary with the gasket. Since this transition is aided by shear, it is possible for the transition to initiate from either location or even both. Grain-level probing would then be necessary to determine internal origins and growth rates.

In addition, there is a need to have theoretical models extend to incorporate other factors related to the kinetics, such as grain size, deformation mechanisms as a function of strain rate, and the role of impurities. The functional form presented by Avrami provides a reasonable starting point to model the resulting compositional data, but the data requires restrictions placed on the exponent to be relaxed. However, our results indicate the current capacity of synchrotron sources for under-

taking such measurements. With further development of the time-resolving capacity of instrumentation, it will become easier to accurately investigate not only the kinetics of such transitions, but also to extend to the kinetics involved with reactions, mixing of liquids, and many other phenomena under pressure that are currently difficult to investigate.

ACKNOWLEDGMENTS

Los Alamos National Laboratory (LANL) is operated by LANS, LLC for the DOE-NNSA under contract no. DE-AC52-06NA25396. The authors acknowledge funding support from LANL Science Campaigns 1 and 2. This work was performed at HPCAT (Sector 16), Advanced Photon Source (APS), Argonne National Laboratory. HPCAT operations are supported by DOE-NNSA under Award No. DE-NA0001974 and DOE-BES under Award No. DE-FG02-99ER45775, with partial instrumentation funding by NSF. APS is supported by DOE-BES, under Contract No. DE-AC02-06CH11357. Use of the Advanced Photon Source, an Office of Science User Facility operated for the US Department of Energy (DOE) Office of Science by Argonne National Laboratory, was supported by the US DOE under Contract No. DE-AC02-06CH11357.

- ¹J. C. Jamieson, *Science* **140**, 2 (1963).
- ²J. Silcock, *Acta Metallurgica* **6**, 481 (1958).
- ³A. Jayaraman, W. Klement, and G. Kennedy, *Physical Review* **131**, 644 (1963).
- ⁴J. Goldak, L. T. Lloyd, and C. S. Barrett, *Physical Review* **144**, 478 (1966).
- ⁵Y. K. Vohra, S. K. Sikka, and R. Chidambaram, *Journal of Physics F: Metal Physics* **9**, 1771 (1979).
- ⁶J. K. Fink and L. Leibowitz, *Journal of Nuclear Materials* **226**, 44 (1995).
- ⁷W. Liu, B. Li, L. Wang, J. Zhang, and Y. Zhao, *Journal of Applied Physics* **104**, 076102 (2008).
- ⁸G. Jyoti, R. Tewari, K. Joshi, D. Srivastava, G. Dey, S. Gupta, S. Sikka, and S. Banerjee, *Defect and Diffusion Forum* **279**, 133 (2008).
- ⁹N. Velisavljevic, G. N. Chesnut, D. M. Dattelbaum, Y. K. Vohra, A. Stemshorn, M. Elert, M. D. Furnish, W. W. Anderson, W. G. Proud, and W. T. Butler, *AIP Conference Proceedings* **1195**, 1213 (2009).
- ¹⁰P. A. Rigg, C. W. Greeff, M. D. Knudson, G. T. Gray, and R. S. Hixson, *Journal of Applied Physics* **106**, 123532 (2009).
- ¹¹H.-R. Wenk, P. Kaercher, W. Kanitpanyacharoen, E. Zepeda-Alarcon, and Y. Wang, *Physical Review Letters* **111**, 195701 (2013).
- ¹²V. D. Blank and E. I. Estrin, *Phase Transitions in Solids Under High Pressure* (CRC Press, Boca Raton, Florida, USA, 2014).
- ¹³J. Zhang, Y. Zhao, P. A. Rigg, R. S. Hixson, and G. T. Gray, *Journal of Physics and Chemistry of Solids* **68**, 2297 (2007).
- ¹⁴N. Velisavljevic, G. N. Chesnut, L. L. Stevens, and D. M. Dattelbaum, *Journal of Physics: Condensed Matter* **23**, 125402 (2011).
- ¹⁵S. K. Sikka, Y. K. Vohra, and R. Chidambaram, *Progress in Materials Science* **27**, 245 (1982).
- ¹⁶H. Xia, A. L. Ruoff, and Y. K. Vohra, *Physical Review B* **44**, 374 (1991).
- ¹⁷A. K. Singh, *Bulletin of Materials Science* **5**, 219 (1983).
- ¹⁸H. Zong, T. Lookman, X. Ding, C. Nisoli, D. Brown, S. R. Niezgoda, and S. Jun, *Acta Materialia* **77**, 191 (2014).
- ¹⁹D. Trinkle, R. Hennig, S. Srinivasan, D. Hatch, M. Jones, H. Stokes, R. Albers, and J. Wilkins, *Physical Review Letters* **91**, 025701 (2003).
- ²⁰D. R. Trinkle, *A theoretical study of the hcp to omega martensitic phase transition in titanium*, Ph.D. thesis, Ohio State University (2003).
- ²¹B. S. Hickman, *Journal of Materials Science* **4**, 554 (1969).
- ²²B. L. Davis and L. H. Adams, *Journal of Geophysical Research* **70**, 433 (1965).
- ²³N. S. Brar, H. H. Schloessin, and R. October, *Canadian Journal of Earth Sciences* **79**, 1402 (1979).
- ²⁴A. Onodera, *Review of Physical Chemistry of Japan* **41**, 1 (1972).
- ²⁵J. Osugi, K. Hara, and M. Katayama, *Bulletin of the Institute for Chemical Research of Kyoto University* **53**, 269 (1975).
- ²⁶C. Divakar, M. Mohan, and A. K. Singh, *Journal of Applied Physics* **56**, 2337 (1984).
- ²⁷A. Singh, *Materials Science Forum* **3**, 291 (1985).
- ²⁸M. Mohan, C. Divakar, and A. K. Singh, *Physica* **139&140B**, 253 (1986).
- ²⁹A. K. Singh, *High Pressure Research* **4**, 336 (1990).
- ³⁰M. Mohan and A. K. Singh, in *Advances in High Pressure Science & Technology*, edited by A. K. Singh (Bangalore, India, 1994).
- ³¹T. Krüger, B. Merkau, W. a. Grosshans, and W. B. Holzapfel, *High Pressure Research* **2**, 193 (1990).
- ³²D.-H. Huang, X.-R. Liu, L. Su, Y. Hu, S.-J. LV, H.-L. Liu, and S.-M. Hong, *Chinese Physics Letters* **24**, 2441 (2007).
- ³³D. H. Huang, X. R. Liu, L. Su, C. G. Shao, R. Jia, and S. M. Hong, *Journal of Physics D: Applied Physics* **40**, 5327 (2007).
- ³⁴M. Avrami, *The Journal of Chemical Physics* **7**, 1103 (1939).
- ³⁵M. Avrami, *The Journal of Chemical Physics* **8**, 212 (1940).
- ³⁶P. J. Clemm and J. C. Fisher, *Acta Metallurgica* **3**, 70 (1955).
- ³⁷J. W. Cahn, *Acta Metallurgica* **4**, 449 (1956).
- ³⁸W. J. Evans, C.-s. Yoo, G. W. Lee, H. Cynn, M. J. Lipp, and K. Visbeck, *The Review of scientific instruments* **78**, 73904 (2007).
- ³⁹N. Velisavljevic, S. Macleod, and H. Cynn, in *Titanium Alloys - Towards achieving enhanced properties for diversified applications* (2008) Chap. 4.
- ⁴⁰W. B. Holzapfel, P. Taylor, and W. B. Holzapfel, *High Pressure Research* **30**, 372 (2010).
- ⁴¹V. L. Solozhenko, O. O. Kurakevych, P. S. Sokolov, and A. N. Baranov, *Journal of Physical Chemistry A* **115**, 4354 (2011).
- ⁴²C.-M. Sung and G. Burns, *Tectonophysics* **31**, 1 (1976).
- ⁴³N. Shankaraiah, K. P. N. Murthy, T. Lookman, and S. R. Shenoy, *Europhysics Letters* **92**, 36002 (2010).
- ⁴⁴D. Errandonea, Y. Meng, M. Somayazulu, and D. Häusermann, *Physica B* **355**, 116 (2005).
- ⁴⁵J. Escobedo, E. Cerreta, C. Trujillo, D. Martinez, R. Lebensohn, V. Webster, and G. Gray, *Acta Materialia* **60**, 4379 (2012).
- ⁴⁶E. K. Cerreta, J. P. Escobedo, P. A. Rigg, F. L. Addessio, T. Lookman, C. A. Bronkhorst, C. P. Trujillo, D. W. Brown, P. O. Dickerson, R. M. Dickerson, and G. T. Gray III, in *Conference proceedings of DYMAT 2012*, Vol. 836 (2012).
- ⁴⁷E. Cerreta, J. Escobedo, P. Rigg, C. Trujillo, D. Brown, T. Sinneros, B. Clausen, M. Lopez, T. Lookman, C. Bronkhorst, and F. Addessio, *Acta Materialia* **61**, 7712 (2013).
- ⁴⁸N. Velisavljevic, M. K. Jacobsen, and Y. K. Vohra, *Materials Research Express* **1**, 035044 (2014).